

Discovery of Coupling between Periodic and Aperiodic Variability and X-ray Quasi-periodic Oscillations from Her X–1

Dae-Sik Moon and Stephen S. Eikenberry

Department of Astronomy, Cornell University, Ithaca, NY 14853
moon,eiken@astrosun.tn.cornell.edu

ABSTRACT

We report the discovery of coupling between periodic and aperiodic variability and ~ 12 -mHz X-ray quasi-periodic oscillations (QPOs) from the X-ray binary pulsar Her X–1 using data from the *Rossi X-Ray Timing Explorer*. We found two different couplings, one during the pre-eclipse dips and the other during the normal state of the source, using a method which directly compares the low-frequency power-density spectra (PDS) with those of the sidebands around the coherent pulse frequency. The pre-eclipse dip lightcurves show significant time variation of photon counts, and this variation appears in the PDS as both strong mHz powers and well-developed sidebands around the coherent pulse frequency. The linear correlation coefficients between the mHz PDS and the sideband PDS obtained from two pre-eclipse dips data segments are 0.880 ± 0.003 and 0.982 ± 0.001 , respectively. This very strong coupling demonstrates that the amplitudes of the coherent pulsations are almost exactly modulated by the aperiodic variabilities, suggesting that both the periodic and aperiodic variabilities are related to time variation of obscuration of X-rays from the central pulsar by an accretion disk during pre-eclipse dips. We also found weak coupling during the normal state of the source, together with ~ 12 -mHz QPOs. The normal state coupling seems to reconcile with the prediction that the aperiodic variabilities from X-ray binary pulsars are due to time-varying accretion flows onto the pulsar’s magnetic poles. If the ~ 12 -mHz QPOs are due to global-normal disk oscillations caused by the gravitational interactions between the central pulsar and the accretion disk, the inferred inner-disk radius is roughly comparable to the magnetospheric radius, $\sim 1 \times 10^8$ cm.

Subject headings: accretion, accretion disks — pulsars: individual (Her X–1) — stars: neutron — X-rays: stars

1. Introduction

Timing analysis of rapid aperiodic variabilities, including quasi-periodic oscillations (QPOs), has been one of the most important tools for studying various types of X-ray binary systems. Since the aperiodic variabilities are generally thought to be related to the innermost motions of accretion

disks, the analysis of aperiodic variabilities can give us useful information about the interaction between accretion disks and the central object in X-ray sources. For example, the power-density spectra (PDS) obtained from observed lightcurves are often used to distinguish between X-ray binary systems containing black holes and neutron stars, to infer rotation rates of neutron stars in low-mass X-ray binary systems, and to investigate accretion-powered X-ray binary pulsars (AXBPs) (e.g., van der Klis 1995).

Among different types of X-ray binaries, AXBPs have unique characteristics in timing analysis. The main time-varying component of AXBPs is periodic coherent pulsations from the central neutron star, and the coexistence of the periodic and aperiodic variabilities makes timing analysis much more complicated than the purely aperiodic cases. This complication often appears as PDS heavily contaminated by numerous bumps and wiggles (van der Klis 1995). On the other hand, detection of periodic coherent pulsations from an X-ray binary makes certain that the compact source is a rotating neutron star. For example, the transient X-ray binary V0332+53 was identified as a neutron star after detection of ~ 4.4 -s periodic coherent pulsations – previously the source had been considered as a black hole candidate because the PDS of the source closely resembles those of the canonical black hole candidate Cyg X–1 (Lazzatti & Stella 1997, and references therein).

Periodic and aperiodic variabilities of AXBPs have usually been studied independently. Recent studies, however, suggest the possibility of coupling between them (Lazzatti & Stella 1997; Burderi et al. 1997), and Moon & Eikenberry (2001) presented an observational evidence in large X-ray flares from the AXBP LMC X–4. It is still not clear, however, exactly when and how the coupling happens. The purpose of this paper is to present another observational example of the coupling in the AXBP Her X–1, together with the discovery of ~ 12 -mHz X-ray QPOs of the source.

Her X–1 is an eclipsing AXBP with pulsational and orbital periods of ~ 1.24 s and ~ 1.7 d, respectively. Its optical companion is a normal star of $\sim 2 M_{\odot}$, making Her X–1 a rare X-ray binary which is not readily classified as a high-mass X-ray binary or a low-mass X-ray binary. Her X–1 has shown very complex temporal features: First, it is one of a few AXBPs showing a superorbital period (~ 35 d), usually ascribed to the motion of a precessing, warped accretion disk periodically obscuring the observer’s line-of-sight to the central neutron star. The ~ 35 -d period consists of at least three sub-states: (1) ~ 7 orbital period main-on state, (2) ~ 5 orbital period short-on state, and (3) two ~ 4 orbital period low states between (1) and (2). Secondly, Her X–1 has shown two different types of dips: pre-eclipse dips and anomalous dips, due to obscuration by the surrounding accretion disk. Thirdly, Her X–1 sometimes shows anomalous low-states (e.g., Coburn et al. 2000). In addition, Her X–1 was recently found to show mHz QPOs in its ultraviolet (UV) continuum, probably emitted on the surface of the companion by reprocessing the X-rays from the neutron star (Boroson et al. 2000).

2. Observations and Analysis

The main-on state of Her X–1 was observed with the *Rossi X-Ray Timing Explorer* (RXTE) on 1996 July 26 and 27 during ~ 27 hours of observation of the source. The photon arrival times from the Good Xenon data of the Proportional Counter Array were transformed to the solar system barycenter using the JPL DE400 ephemeris. Sixteen data segments, each with lengths of 0.5–1 h, including five segments of pre-eclipse dips were obtained.

2.1. Pre-Eclipse Dips

Two lightcurves of the pre-eclipse dips, obtained with the five RXTE Proportional Counter Units in 2–30 keV energy range, are shown in Fig. 1 with 4-s time resolution. The strong aperiodic variabilities are clearly identified in Fig. 1, and we shall call the two lightcurves “PED 1” and “PED 2”, respectively. The phase of the ~ 35 -d super-orbital motion, based on the ephemeris of Scott & Leahy (1999), is ~ 0.125 , while the ~ 1.7 -d binary orbital phases, based on the ephemeris of Deeter et al. (1991), of PED 1 and PED 2 are ~ 0.84 and ~ 0.88 , respectively. The Leahy-normalized PDS of the lightcurves obtained with 2^{-6} s time resolution are presented in Figure 2. Only the first ~ 0.71 -h data of PED 1 were used in order to avoid data gaps, while the full ~ 0.92 -h data were used for PED 2. Fig. 2 shows the PDS around the coherent pulse frequency (~ 0.81 Hz) in the main window, the low-frequency (mHz) PDS in the small windows on the left side (in the logarithmic frequency scale), and the detailed structures of the sidebands around the coherent frequency in the small windows on the right side. Three characteristics are evident in the PDS of Fig. 2: (1) a strong peak at the coherent pulse frequency, (2) well-developed significant sidebands around the coherent frequency, and (3) strong low-frequency variability at ~ 1 –10 mHz. The rms fractions of the low-frequency components are $\sim 30 \pm 5$ % and $\sim 64 \pm 10$ % for PED 1 and PED 2, respectively, while those of the coherent pulsations ($\nu = 0.795$ – 0.820 Hz including the sidebands) are $\sim 47 \pm 5$ % for both PED 1 and PED 2.

The mHz powers and the sidebands around the coherent frequency in Fig. 2 are compared in Fig 3, where the mHz powers are overlaid onto the sidebands as follows: First, the mHz powers are shifted to the frequency of the higher-frequency (HF) sidebands, and then a lower-frequency (LF) mirror image was made with respect to the coherent frequency. Finally, the shifted mHz powers are scaled to match the sidebands. In Fig. 3, very similar distributions between the shifted, scaled mHz powers (crosses) and the sidebands (solid histogram) are identified, indicating that the amplitudes of periodic coherent pulsations are modulated by those of the aperiodic variabilities (or vice versa). Linear correlation coefficients between them are 0.880 ± 0.003 and 0.982 ± 0.001 over 74 and 78 bins for PED 1 and PED 2, respectively. We estimated the uncertainties in the correlation coefficients using a Monte Carlo simulation, creating 1000 simulated sideband/mHz power distributions. Each simulated distribution had 74 (for PED 1; 78 for PED 2) Fourier bins drawn with replacement from the actual sideband/mHz power distributions. The quoted uncertainties are the maximum

deviations from the actual correlation coefficients over these 1000 simulations, and thus correspond approximately to 99.9% confidence level. We performed an additional Monte Carlo simulation as a null test, scrambling the order of the mHz powers while maintaining the order of the sideband powers. This resulted in average correlation coefficients of 0.007 and -0.001 respectively for PED 1 and PED 2, with standard deviations of 0.114 in each case, confirming that the observed correlations are statistically significant.

2.2. Normal State

We show the lightcurve, PDS, and comparison between the shifted, scaled mHz powers and the sidebands around the pulse frequency of a ~ 0.7 -h gapless data segment obtained during the normal state in Figure 4. Initial orbital phase of the data segment is ~ 0.22 . The strong aperiodic variabilities (and the corresponding large mHz powers), which have been seen in Fig. 1 and 2 during pre-eclipse dips, are absent in Fig 4; however, there exists a relatively weak (compared to the pre-eclipse dips) correlation between the shifted, scaled mHz powers and the sidebands in Figure 4(c). A linear correlation coefficient, obtained by fitting 62 bins, is 0.492 ± 0.020 , which is much smaller than those of the pre-eclipse dips but still indicates a statistically significant (i.e., ~ 95 % confidence level) correlation. A linear correlation coefficient between randomly sampled mHz powers and sidebands are -0.002 ± 0.126 .

Fig. 5 shows the averaged PDS (solid histogram) of the normal state obtained by averaging the PDS of 13 gapless data segments of 1200-s length. The most conspicuous feature in Fig. 5 is the increase of the power intensity at the low-frequency range (i.e., red noise) with an excess component at $\nu \simeq 12$ mHz. The PDS at $\nu < 0.03$ Hz were analyzed by χ^2 -fitting in two different ways. First, a power-law component and a Lorentzian component were assumed for the red noise and the excess component in the fitting. Next, instead of the power-law component, a Gaussian component (centered at $\nu = 0$ Hz) and a Lorentzian component were used. In both fittings, a background power intensity 38 was assumed, which is evident from the PDS at higher frequency. While the reduced χ^2 from the first method is ~ 2.5 , the value from the second method is ~ 0.98 , both with 15 degree of freedom. It is worth, at this point, to note that the red noise in Fig. 5 does not seem to follow a power-law distribution, which has been frequently assumed as the red noise distribution in the literature. The PDS in Fig. 5 in fact seems to indicate the existence of another component at $\nu \simeq 5$ mHz. Although another component might exist, the short time duration (i.e., poor frequency resolution) of our data segments makes it impossible to resolve the component. The central frequency and full width half maximum (FWHM) of the Lorentzian component obtained with the second method are 12.4 ± 2.2 mHz and 4.9 ± 3.5 mHz, respectively. The uncertainties correspond to ~ 68.3 % confidence level. The results of the fitting is presented in Fig. 5 (dotted histogram). The symmetric distribution and relative width (FWHM/central frequency) of the excess component seem to satisfy the condition of being acknowledged as QPOs (van der Klis 1995). A signal to noise ratio of ~ 3.3 was obtained for the QPOs in Fig. 5 using the method

described by Boirin et al. (2000). The rms fraction of the QPOs was calculated to be $\sim 1.7 \pm 0.6$ % over the FWHM. The central frequency, width, and rms fraction of the QPOs are roughly comparable to the $\sim 8 \pm 2$ mHz UV QPOs (Boroson et al. 2000).

3. Discussion

3.1. Coupling between Periodic and Aperiodic Variability

It is reasonable to attribute the origin of the strong aperiodic variabilities in the pre-eclipse dips to the variation of obscuration due to an inhomogeneous distribution of the absorbing material in the accretion disk, integrated along the observer’s line-of-sight to the central pulsar. This, together with the very strong correlations between the mHz powers and the sidebands, imply that both the amplitudes of the aperiodic variabilities and the amplitude changes of the periodic coherent pulsations are proportional to the same parameter: the amount of obscuration of the X-ray beam from the pulsar by the accretion disk during the pre-eclipse dips.

Although most of previous studies have treated the periodic and aperiodic variabilities independently, we might expect the coupling between them because most of the aperiodic variabilities are due to the time-varying funneling of the accreting columns onto the magnetic poles of the pulsars and, subsequently, the aperiodic variabilities should be modulated by the pulsar rotations. Recently, Lazzati & Stella (1997) and Burderi et al. (1997) have demonstrated models with correlations between the PDS broadening of the wings around coherent peaks and the red-noise components, indicating couplings between the periodic and aperiodic variabilities. The results also cast doubt on the reported apparent correlation between the pulse frequency and the knee frequency, below which the PDS steepens, of X-ray pulsars (Lazzati & Stella). The correlation between the mHz powers and sidebands found in the normal state of Her X–1 in this study seems to be consistent with the results (Lazzati & Stella 1997; Burderi et al. 1997), which predict the origin of the aperiodic variabilities (i.e., red noise) to be the accretion flows near the stellar surface.

3.2. The X-ray QPOs

The global-normal disk oscillations model (GDOM), which is recently proposed by Titarchuk & Osherovich (2000), seems to be capable of accounting for the ~ 12 -mHz X-ray QPOs. In GDOM, ~ 0.01 – 1 Hz persistent oscillations reported in several X-ray binaries can be produced in the accretion disks surrounding the compact X-ray sources as a result of the gravitational interaction between the central sources and the accretion disks. The oscillation frequency is a function of several parameters including inner-disk radius (R_{in}), outer-disk radius (R_{out}), adjustment radius (R_{adj} , below which surface density is assumed to be constant), power index of the surface density distribution (γ), and mass of the central source (M_X). The expected inner-disk radius of Her X–1

responsible for the X-ray QPOs is given by

$$R_{\text{in}} \simeq 3.1 \times 10^5 \nu_{\text{QPO}}^{-5/4} \text{ cm} \quad (1)$$

where ν_{QPO} is in unit of Hz. We have used $R_{\text{out}} = 1.7 \times 10^{11}$ cm (Howarth & Wilson 1983), $R_{\text{adj}} = 3 R_{\text{in}}$ and $\gamma = 3/5$ (Titarchuk & Osherovich), and $M_X = 1.4 M_{\odot}$. The resulting inner-disk radius corresponding to the ~ 12 mHz QPOs is $R_{\text{in}} \simeq 0.5\text{--}1.3 \times 10^8$ cm.

For the case of AXBPs with strong magnetic field strength ($B \sim 10^{12}$ G), such as Her X–1, the magnetic field is expected to disrupt the inner accretion disk around the magnetospheric radius, $r_M \simeq \xi r_A$, where ξ is a dimensionless parameter of ≤ 1 and r_A is the Alfvén radius at which magnetic pressure is in equilibrium with gas pressure (Shapiro & Teukolsky 1983; Bildsten 1997). Using X-ray luminosity $L_X \simeq 2.1 \times 10^{37}$ ergs s $^{-1}$ (Choi et al. 1994), the assumed neutron star radius $R = 1 \times 10^6$ cm, and the magnetic field strength $B \simeq 3 \times 10^{12}$ G estimated from the analysis of cyclotron resonance features (Makishima et al. 1999, and references therein), we obtain $r_A \simeq 5.4 \times 10^8$ cm for an $1.4 M_{\odot}$ neutron star. If we consider various assumptions used in obtaining the Alfvén radius (e.g., Shapiro & Teukolsky) and in the GDOM, the expected magnetospheric radius seems to be roughly comparable to the inner-disk radius of the GDOM calculated above. (We note that Titarchuk & Osherovich [2000] accounted for the 48 ± 2 mHz UV QPOs of Her X–1 by assuming $R_{\text{in}} \simeq 1 \times 10^7$ cm, which is much smaller than the magnetospheric radius. It was not explained, however, how the inner disk can penetrate the strong magnetospheric barrier of Her X–1 to near the surface of the central pulsar.)

On the other hand, Boroson et al. (2000) discussed in detail the 8 ± 2 mHz UV QPOs from Her X–1 in terms of two canonical models for QPOs, the beat-frequency model and the Keplerian-frequency model. According to them, the UV QPO frequency, in principle, can be explained by either the BFM or the KFM. Since the frequency is comparable to the frequency of the normal-state X-ray QPOs of this study, we ascribe the detailed discussion of the origin of the normal-state QPOs via these models to Boroson et al. (2000).

4. Conclusions

The results of this paper are summarized as follows:

- We have discovered coupling between the periodic aperiodic variabilities from the AXBP Her X–1 when the source is in the pre-eclipse dip and normal state, respectively. The coupling suggests that the amplitudes of the periodic coherent pulsations are modulated by the amplitudes of the aperiodic variabilities.
- The coupling in pre-eclipse dips indicates that both the periodic and aperiodic variabilities are related to the same parameter: the amount of obscuration of X-ray beam from the pulsar by the accretion disk during the pre-eclipse dips.

- The normal state coupling may indicate that the aperiodic variabilities from X-ray binary pulsars are due to time-varying accretion flows onto the pulsar’s magnetic poles.
- We have also discovered ~ 12 -mHz X-ray QPOs which are comparable to the previously detected UV QPOs from the source.
- If the ~ 12 -mHz X-ray QPOs are due to the global-normal disk oscillations caused by the gravitational interactions between the central pulsar and the accretion disk, the inferred inner-disk radius is roughly comparable to the magnetospheric radius, $\sim 1 \times 10^8$ cm.
- The results of this paper, together with our previous results on LMC X–4 (Moon & Eikenberry 2001), offer unique opportunities for studying timing behaviour of accretion-powered X-ray binary pulsars.

We would like to thank the anonymous referee for comments and suggestions which substantially improved this paper. DSM acknowledges Wynn Ho for his careful reading of manuscript and comments. This research has made use of data obtained from the *High Energy Astrophysics Science Archive Research Center* (HEASARC), provided by NASA’s Goddard Space Flight Center. DSM is supported by NSF grant AST-9986898. SSE is supported in part by an NSF Faculty Early Career Development (CAREER) award (NSF-9983830).

REFERENCES

- Bildsten, L. et al. 1997, *ApJS*, 113, 367
- Boirin, L., Barret, D., Olive, J. F., Bloser, P. F., & Gindlay, J. E. 2000, *A&A*, 361, 121
- Boroson, B., O’Brien, K., Horne, K., Kallman, T., Still, M., Boyd, P. T., Quaintrell, H., & Vrtillek, S. D. 2000, *ApJ*, 545, 399
- Burderi, L., Robba, N. R., La Barbera, N., & Guainazzi, M. 1997, *ApJ*, 481, 943
- Choi, C. S., Nagase, F., Makino, F., Dotani, T., & Min, K. W. 1994, *ApJ*, 422, 799
- Coburn, W., et al. 2000, *ApJ*, 543, 351
- Deeter, J. E., Boynton, P. E., Miyamoto, S., Kitamoto, S., Nagase, F., & Kawai, N. 1991, *ApJ*, 383, 324
- Howarth, I. D., & Wilson, B. 1983, *MNRAS*, 202, 347
- Lazzati, D., & Stella, L. 1997, *ApJ*, 476, 267
- Makishima, K., Mihara, T., Nagase, F., & Tanaka, Y. 1999, *ApJ*, 525, 978

Moon, D.-S., & Eikenberry, S. S. 2000, ApJL, in press

Scott, D. M., & Leahy, D. A. 1999, ApJ, 510, 974

Shapiro, S. L., & Teukolsky, S. A. 1983 Black Holes, White Dwarfs, and Neutron Stars: The Physics of Compact Objects (USA: John Wiley & Sons), 451

Titarchuk, L., & Osherovich, V. 2000, ApJ, 542, L111

van der Klis, M. 1995, in X-Ray Binaries, ed. W. H. G. Lewin, J. van Paradijs, & E. P. J. van den Heuvel (Cambridge: Cambridge Univ. Press), 252

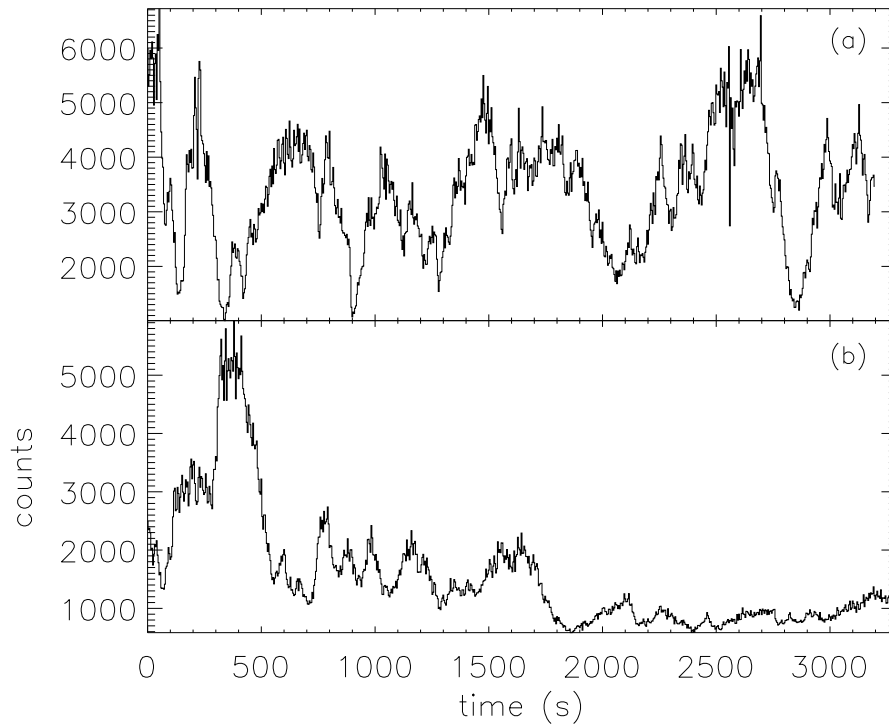


Fig. 1.— Lightcurves, in 2–30 keV energy range with 4-s time resolution, of Her X–1 during pre-eclipse dips : (a) for PED 1 and (b) for PED 2.

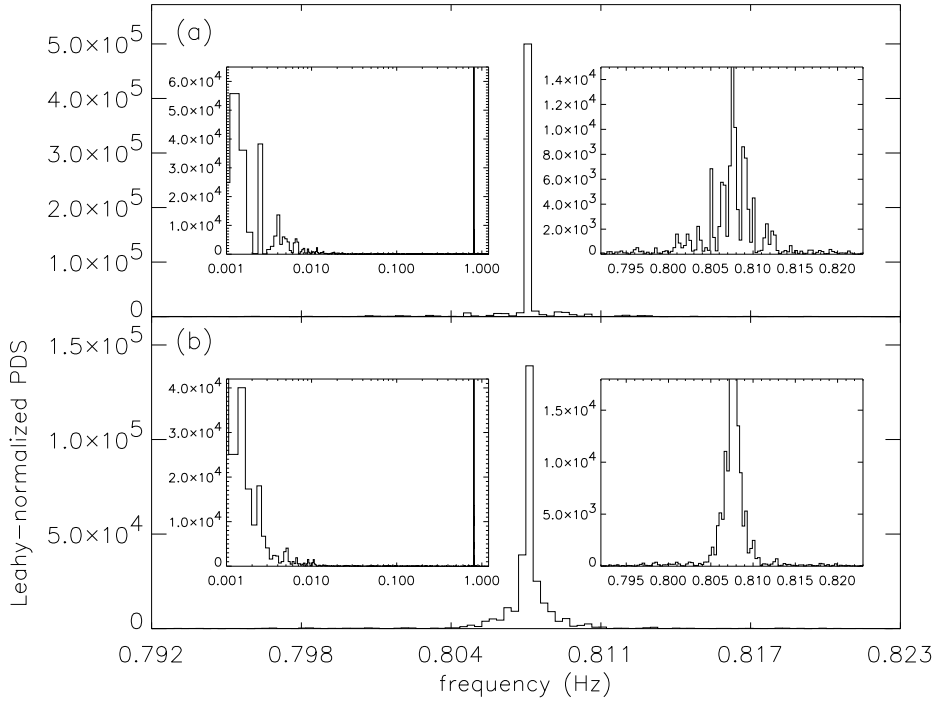


Fig. 2.— Power-density spectra (PDS) of the lightcurves in Fig. 1: (a) PED 1 and (b) PED 2. The main windows show the PDS around the coherent pulse frequency. The small windows on the left side show the mHz PDS in the logarithmic frequency scale, while the small windows on the right side show the detailed structures of the sidebands around the coherent frequency.

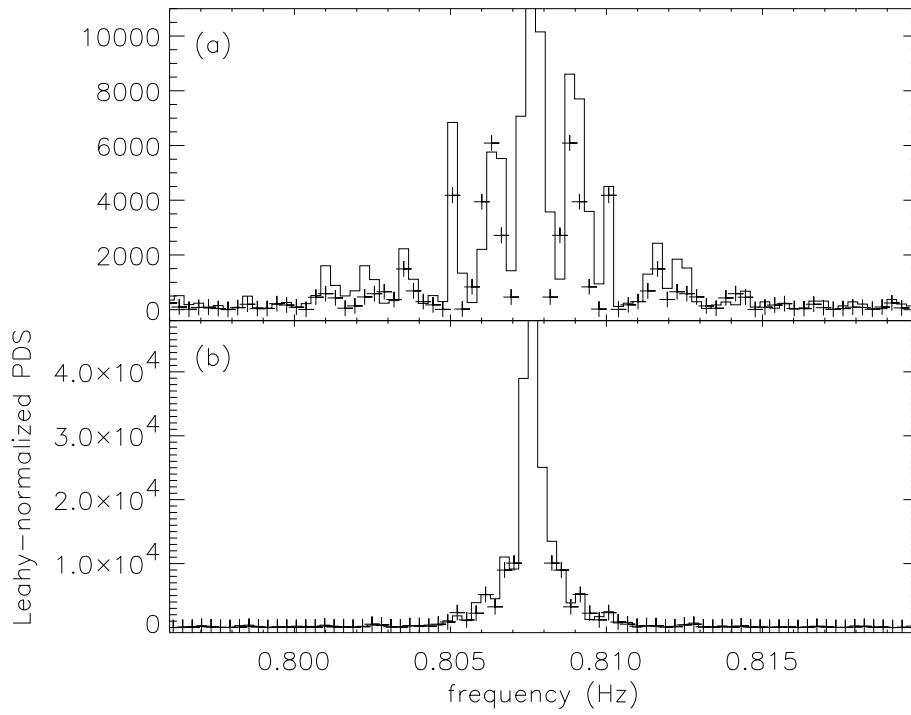


Fig. 3.— (a) Comparison between the PDS of the sidebands (solid histogram) and the shifted, scaled PDS (crosses) of the mHz QPOs for (a) PED 1 and (b) PED 2.

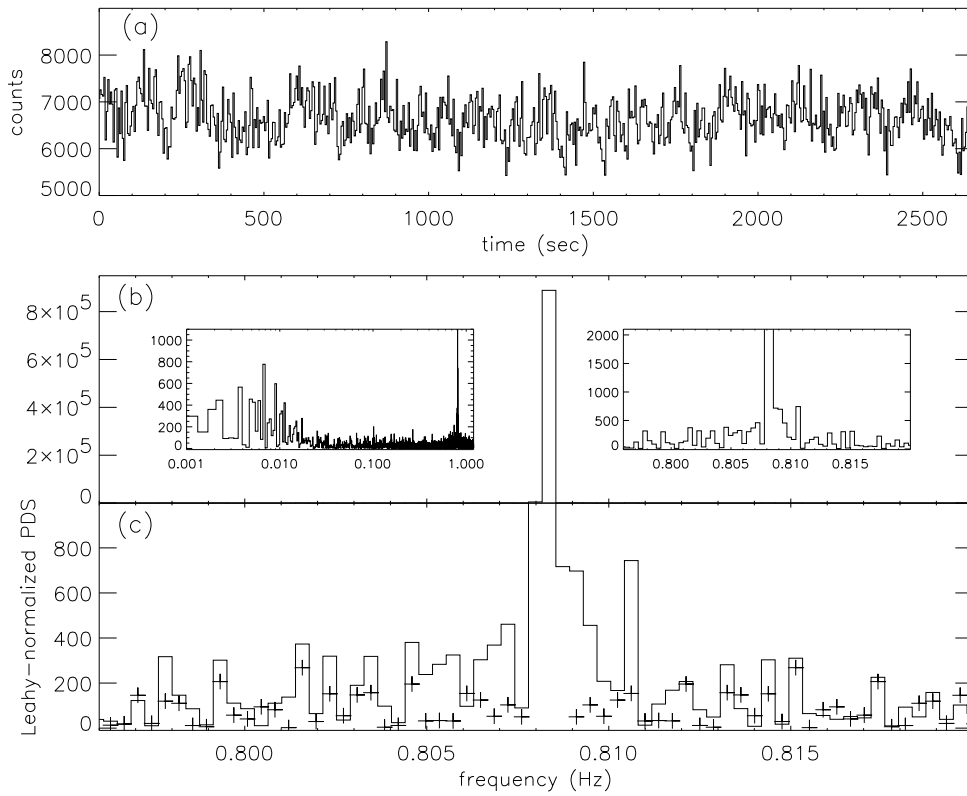


Fig. 4.— (a) Same as Fig. 1, but for the ~ 0.7 -h gapless data segment of the normal state. (b) Same as Fig. 2, but for the lightcurve of (a). (c) Same as Fig. 3, but for the PDS of (b).

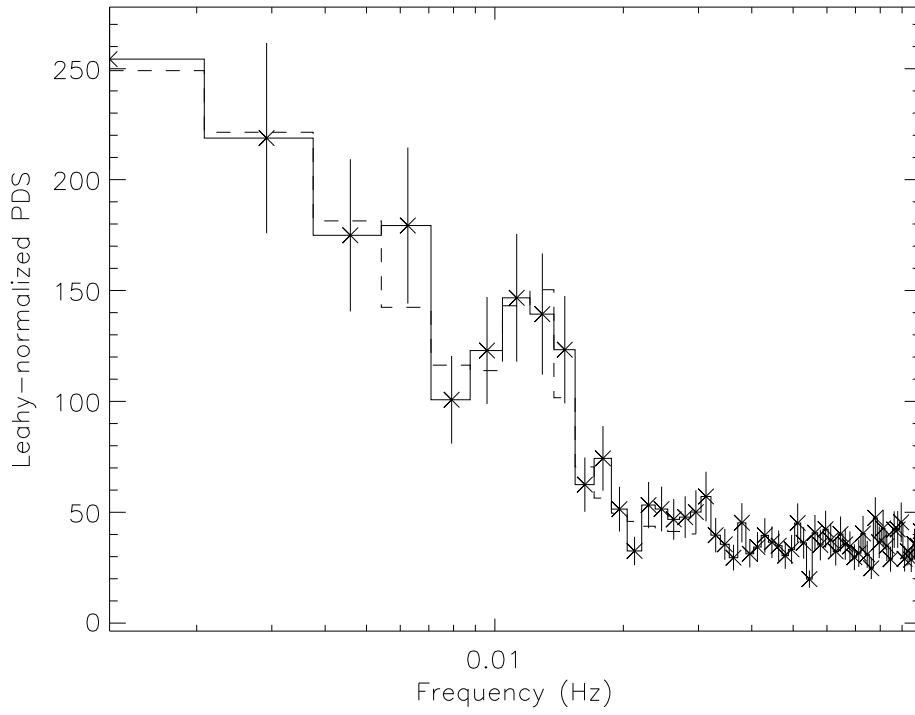


Fig. 5.— Superposition of the PDS of the normal state (solid histogram) obtained by averaging PDS of 13 data segments of 1200-s length on the PDS obtained by fitting the averaged PDS with one Gaussian component and one Lorentzian component (dotted histogram). The error bars represent $\sim 68.3\%$ confidence level.